5th International Symposium on Three-Dimensional Electromagnetics
Sapporo, Japan, May 7–9, 2013

Inversion of large scale airborne time domain electromagnetic data

Christoph Schwarzbach and Eldad Haber
University of British Columbia, Vancouver, Canada

SUMMARY

3-D inversion of airborne electromagnetic data is, to date, a challenging computational problem. The size of the survey area in relation to the desired spatial resolution of subsurface electrical resistivity as well as the mesh size that is required to adequately discretize all transmitters and receivers give rise to very large meshes. Solving the forward problem repeatedly on such a mesh either requires intense computational resources or is simply infeasible. However, using a single mesh for both the inverse problem and the forward problem for all transmitters is not necessary. The forward problem for a single source or a small group of sources can as well be solved on a much smaller mesh which only needs to be fine close to the selected transmitters and receivers. Away from transmitters and receivers the mesh can be coarse. The forward problem is, thus, broken into a number of smaller problems which are easier and faster to solve. In this paper, we present an implementation of this idea using a finite volume discretization on OcTree meshes. We demonstrate our approach with a synthetic example involving 4064 transmitters.

Keywords: forward modeling, inversion, finite volume, airborne EM

INTRODUCTION

The airborne electromagnetics (AEM) inverse problem constitutes finding the spatial distribution of subsurface electrical resistivity ρ which explains observed data within the limits of data uncertainty. To find such an earth model ρ, we need to be able to compute predicted data given ρ. This is the solution of the forward problem. Solving the forward problem for AEM surveys we face a number of challenges. The first one is the large number of sources to be considered. The airborne AEM system, consisting of a single transmitter and a single receiver, is moved across the survey area by an aircraft and can rapidly acquire data at thousands to millions of locations. Typically, the time to solve the forward problem scales linearly with the number of sources. Therefore, we have to find an efficient way to solve the forward problem.

The second problem is a problem of scales. AEM surveys can cover large areas and aim at resolving both small- and large-scale variations of the subsurface resistivity. To this end, we introduce a mesh $\mathscr{S}^H$ which subdivides the subsurface into cells and we seek to find the (constant) resistivity value in each of the cells. $\mathscr{S}^H$ needs to cover the whole survey area to consistently account for large-scale features. At the same time, its cell size needs to be fine enough to recover the small-scale features and to reflect the spatial resolution of the data. This easily leads to meshes with millions of cells. While $\mathscr{S}^H$ is designed for solving the inverse problem, it is inadequate for solving the forward problem. To solve the forward problem for the i-th transmitter–receiver pair, the local nature of the measurement asks for a mesh $\mathscr{S}_i^h$ which is fine only in the vicinity of the transmitter and the receiver and which can be coarse elsewhere. Such a mesh involves far fewer cells than $\mathscr{S}^H$. Reducing the number of cells greatly accelerates the solution of the forward problem: the linear solvers involved scale superlinearly with the number of unknowns. A smaller forward problem mesh $\mathscr{S}_i^h$, in fact, makes feasible solution approaches which are infeasible if $\mathscr{S}^H$ is used, like direct solvers and storage of sensitivities.

In this paper, we present the implementation of an inversion algorithm which uses the globally fine mesh $\mathscr{S}^H$ to solve the inverse problem and locally fine meshes $\mathscr{S}_i^h$, $i = 1,2,\ldots$ to solve the forward problem for selected transmitter–receiver pairs. $\mathscr{S}_i^h$ can be chosen to accommodate just a single source or a group of sources that are close by. Despite increasing the number of cells, grouping sources might lead to an overall faster execution time because the total number of meshes, the total memory footprint and some computational overhead is reduced.

This extends our previous work on time domain electromagnetics inversion using a single regular (tensor-product) mesh (Haber, Oldenburg, & Shektman, 2007) to multiple OcTree meshes. The underlying regular structure of OcTree meshes greatly simplifies mesh handling and algorithmic development, compared to the finite element method on unstructured tetrahedral meshes (Günther, Rücker, & Spitzer, 2006; Schwarzbach, Börner, & Spitzer, 2011; Schwarzbach & Haber, 2013). A similar approach has been published by Cox & Zhdanov (2008)

using integral equations. While Cox & Zhdanov (2008) simply truncate the computational domain to solve the forward problem for a particular source, we discretize the whole domain, albeit with rather coarse cells, and homogenize the resistivity of fine cells of $\mathscr{S}^H$ to obtain a value for coarse cells of $\mathscr{S}_i^h$. Our approach, however, offers the flexibility to adjust the cell size and take large conductors (like the ocean) into account which can influence the measurement even from a large distance.

FORWARD PROBLEM

We formulate the forward problem as an initial boundary value problem in terms of the magnetic field, that is, we seek $\boldsymbol{H}_i(\boldsymbol{x},t)$ such that

$$\nabla\times(\rho(\boldsymbol{x})\nabla\times\boldsymbol{H}_i(\boldsymbol{x},t))+\mu(\boldsymbol{x})\partial_t\boldsymbol{H}_i(\boldsymbol{x},t)= \nabla\times\big(\rho(\boldsymbol{x})\nabla\times\boldsymbol{H}_{i,0}(\boldsymbol{x})\hat{I}(t)\big), \quad (1a)$$

for $\boldsymbol{x}\in\Omega$ and $t\in(0,T]$ subject to the initial condition

$$\boldsymbol{H}_i(\boldsymbol{x},0)=\boldsymbol{H}_{i,0}(\boldsymbol{x}) \quad (1b)$$

and subject to the boundary condition

$$\boldsymbol{n}\times(\rho(\boldsymbol{x})\nabla\times\boldsymbol{H}_i(\boldsymbol{x},t))=\boldsymbol{0} \quad (1c)$$

for $\boldsymbol{x}\in\partial\Omega$. As usual, ρ denotes electrical resistivity and μ magnetic permeability. The subscript i indicates the i-th transmitter. We model the transmitter by a current loop which carries a current $I(t)$. For $t\le 0$, we assume that $I(t)=I_0$ is constant, giving rise to the magnetostatic field $\boldsymbol{H}_{i,0}(\boldsymbol{x})$ which satisfies, in particular, $\nabla\cdot(\mu(\boldsymbol{x})\boldsymbol{H}_{i,0}(\boldsymbol{x}))=0$. At $t=0$, the current is shut off instantaneously or gradually which is reflected by the function $\hat{I}(t)=I(t)/I_0$.

We discretize the initial boundary value problem (1) in space using the finite volume method on OcTree meshes (Haber & Heldmann, 2007; Horesh & Haber, 2011) and in time using the backward Euler method. This yields a system of linear equations which can be written in compact form as

$$\mathbf{A}_i(\boldsymbol{m})\boldsymbol{u}_i=\boldsymbol{b}_i(\boldsymbol{m}) \quad (2)$$

where

$$\mathbf{A}_i(\boldsymbol{m})=\begin{pmatrix}\mathbf{M}_i+\delta t_1\mathbf{K}_i(\boldsymbol{m}) & & & \\ -\mathbf{M}_i & \mathbf{M}_i+\delta t_2\mathbf{K}_i(\boldsymbol{m}) & & \\ & \ddots & \ddots & \\ & & -\mathbf{M}_i & \mathbf{M}_i+\delta t_n\mathbf{K}_i(\boldsymbol{m})\end{pmatrix},$$

$$\boldsymbol{u}_i=\begin{pmatrix}\boldsymbol{h}_{i,1}\\ \boldsymbol{h}_{i,2}\\ \vdots\\ \boldsymbol{h}_{i,n}\end{pmatrix} \quad \text{and}$$

$$\boldsymbol{b}_i(\boldsymbol{m})=\begin{pmatrix}(\mathbf{M}_i+\delta t_1 f_1\mathbf{K}_i(\boldsymbol{m}))\boldsymbol{h}_{i,0}\\ \delta t_2 f_2\mathbf{K}_i(\boldsymbol{m})\boldsymbol{h}_{i,0}\\ \vdots\\ \delta t_n f_n\mathbf{K}_i(\boldsymbol{m})\boldsymbol{h}_{i,0}\end{pmatrix}.$$

Here, $\mathbf{M}_i$ is the mass matrix resulting from the finite volume discretization of the time derivative term in eq. (1a) and $\mathbf{K}_i$ is the discrete counterpart of the differential operator $\nabla\times(\rho(\boldsymbol{x})\nabla\times\cdot)$. The subscript i indicates that the discretization depends on the mesh $\mathscr{S}_i^h$. $\delta t_1,\dots,\delta t_n$ are the time step lengths. The vectors $\boldsymbol{h}_{i,0},\boldsymbol{h}_{i,1},\dots,\boldsymbol{h}_{i,0}$ contain the tangential magnetic field components at the edges of the OcTree mesh at times $t_0,t_1,\dots,t_n$. $f_1,\dots,f_n$ are the values of $f(t)$ at times $t_1,\dots,t_n$. Note that the right-hand side $\boldsymbol{b}_i$ depends on the model parameter vector $\boldsymbol{m}$ if the source is active during time stepping, that is, if any $f_1,\dots,f_n$ is nonzero.

The model parameter vector $\boldsymbol{m}$ is defined on the global mesh $\mathscr{S}^H$ and contains the log-resisitivity of each cell of $\mathscr{S}^H$. To obtain the resistivity for the cells of the i-th local mesh $\mathscr{S}_i^h$, we introduce an operator $\mathscr{P}_i:\mathscr{S}^H\to\mathscr{S}_i^h$ which maps the resisitivity values of the global OcTree cells to values of the local OcTree cells. A simple solution for this homogenization problem is taking the volume-weighted average of resistivity. This reduces $\mathscr{P}_i$ to the averaging matrix $\mathbf{P}_i$ and leaves us with the expression $\mathbf{P}_i\exp(\boldsymbol{m})$ for the vector of resistivity values on the local mesh $\mathscr{S}_i^h$.

Solving eq. (2) involves solving n systems of linear equations with the system matrices $\mathbf{M}_i+\delta t_k\mathbf{K}_i(\boldsymbol{m})$ $(k=1,\dots,n)$. Since the forward problem is discretized on the small local mesh $\mathscr{S}_i^h$, the use of sparse direct solvers becomes feasible. They are preferrable to iterative solvers, in particular, if the factorization can be reused for time steps of the same length or multiple sources accommodated by the same mesh.

In a standard AEM survey, the time derivative of the vertical magnetic induction $\partial B_z/\partial t$ is measured. Denote by $d_{i,j}^{obs}$ the observed value of $\partial B_z/\partial t$ at the i-th transmitter/receiver location and at the j-th time channel. The predicted data can be computed from $\boldsymbol{u}_i$ by finite differencing in time and interpolation in space and time. For time channel j and source–receiver pair i we have

$$d_{i,j}(\boldsymbol{m})=\boldsymbol{q}_{i,j}^\top\boldsymbol{u}_i=\boldsymbol{q}_{i,j}^\top[\mathbf{A}_i(\boldsymbol{m})]^{-1}\boldsymbol{b}_i(\boldsymbol{m}) \quad (3)$$

where the vector $\boldsymbol{q}_{i,j}$ contains the interpolation weights and finite difference coefficients.

INVERSE PROBLEM

To match the predicted and the observed data, we solve a minimization problem and seek a model vector $\boldsymbol{m}^*$ such that

$$\boldsymbol{m}^*=\arg\min_{\boldsymbol{m}}\phi(\boldsymbol{m}), \quad (4a)$$

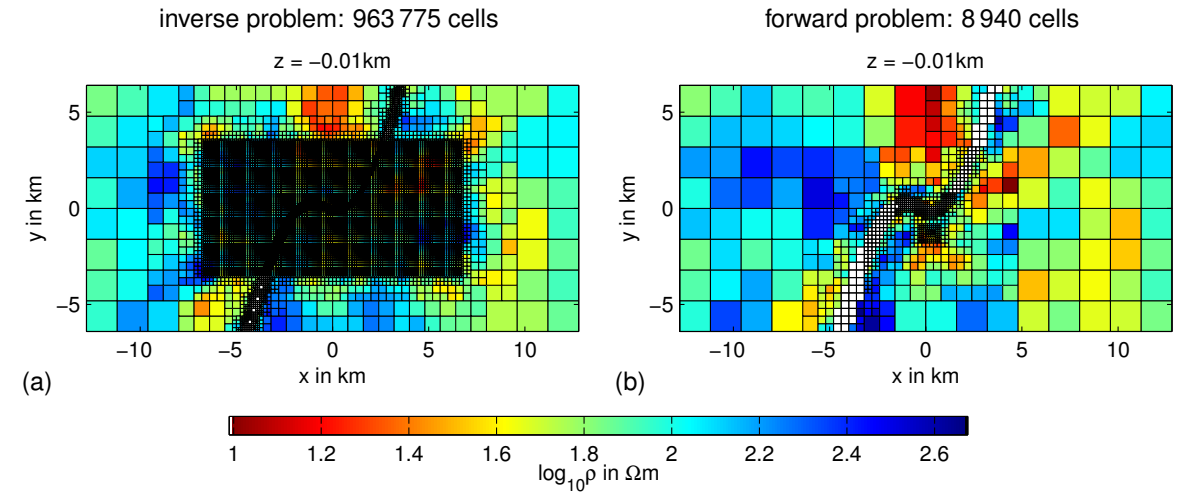

Figure 1. Horizontal slices through the inverse problem mesh (a) and through one of the forward problem meshes (b). The forward problem mesh is locally refined only near three transmitters/receivers at $x = 0.1\,\text{km}$ to $0.3\,\text{km}$, $y = -1.3\,\text{km}$ and at a topographic feature close by.

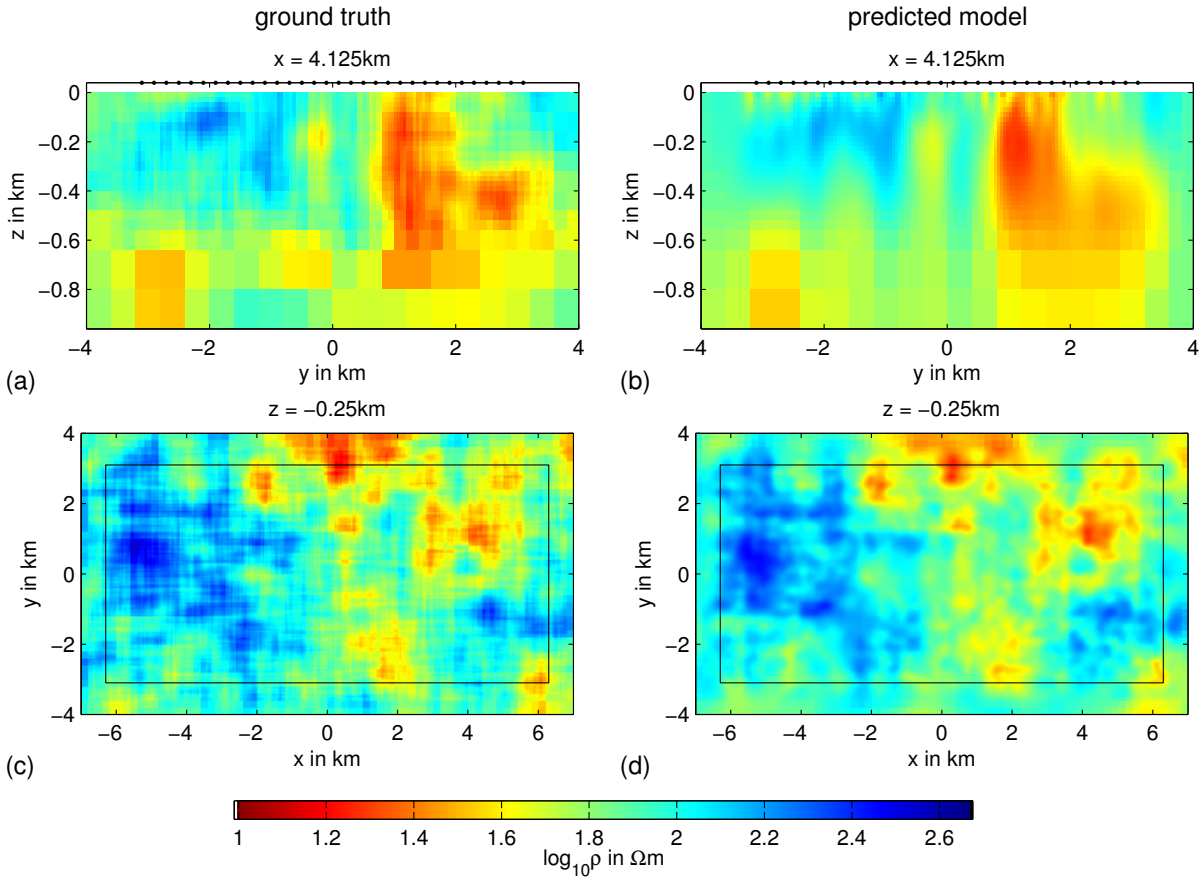

Figure 2. Vertical (a, b) and horizontal (c, d) slices of log-resistivity of the ground truth (a, c) and of the predicted model (b, d). The dots at $z = 40\,\text{m}$ (a, b) and the black rectangle (c, d) indicate the location of the survey area.

where

$$\phi(\boldsymbol{m}) = F(\boldsymbol{m}) + \alpha R(\boldsymbol{m}), \tag{4b}$$

$$F(\boldsymbol{m}) = \sum_{i=1}^{n_s}\sum_{j=1}^{n_t}\left(\frac{d_{i,j}(\boldsymbol{m}) - d_{i,j}^{obs}}{\sqrt{n_s n_t}\, d_{i,j}^{std}}\right)^2, \tag{4c}$$

n_s denotes the number of sources, n_t the number of measured time channels, $d_{i,j}^{std}$ the standard deviation of datum $d_{i,j}^{obs}$, α the regularization parameter and $R(\boldsymbol{m})$ a smoothness regularization functional.

To minimize the non-linear objective function $\phi(\boldsymbol{m})$ we use the Gauss-Newton method. Given an initial model $\boldsymbol{m}_0$, this involves, for $\ell = 1, 2, \ldots$, computing the Gauss-Newton direction $\delta\boldsymbol{m}_\ell$ from

$$\begin{aligned}&\left(\mathbf{J}(\boldsymbol{m}_{\ell-1})^\top \mathbf{J}(\boldsymbol{m}_{\ell-1}) + \alpha \mathbf{R}^\top \mathbf{R}\right)\delta\boldsymbol{m}_\ell = \\ &-\mathbf{J}(\boldsymbol{m}_{\ell-1})^\top \boldsymbol{r}(\boldsymbol{m}_{\ell-1}) - \alpha \mathbf{R}^\top \mathbf{R}\left(\boldsymbol{m}_{\ell-1} - \boldsymbol{m}_{ref}\right)\end{aligned} \tag{5a}$$

and updating the model

$$\boldsymbol{m}_\ell = \boldsymbol{m}_{\ell-1} + \zeta_\ell \delta\boldsymbol{m}_\ell \tag{5b}$$

where the step length control $\zeta_\ell \leq 1$ is chosen such that $\phi(\boldsymbol{m})$ is reduced sufficiently. The residual vector $\boldsymbol{r}(\boldsymbol{m})$ and the sensitivity matrix $\mathbf{J}(\boldsymbol{m})$ are

$$\boldsymbol{r}(\boldsymbol{m}) = \begin{pmatrix} r_{1,1}(\boldsymbol{m}) & \ldots & r_{n_s,n_t}(\boldsymbol{m})\end{pmatrix}^\top, \tag{6a}$$

$$r_{i,j}(\boldsymbol{m}) = \frac{d_{i,j}(\boldsymbol{m}) - d_{i,j}^{obs}}{\sqrt{n_s n_t}\, d_{i,j}^{std}}, \tag{6b}$$

$$\mathbf{J}(\boldsymbol{m}) = \begin{pmatrix} \boldsymbol{j}_{1,1}(\boldsymbol{m}) & \ldots & \boldsymbol{j}_{n_s,n_t}(\boldsymbol{m})\end{pmatrix}^\top, \tag{6c}$$

$$\boldsymbol{j}_{i,j}(\boldsymbol{m}) = \nabla_{\boldsymbol{m}} r_{i,j}(\boldsymbol{m}). \tag{6d}$$

By virtue of the chain rule the sensitivity matrix can be reduced to the product of the homogenization matrix $\mathbf{P}_i$ with local sensitivity matrices, that is, the sensitivity of $r_{i,j}(\boldsymbol{m})$ to changes of resistivity in the local mesh ($\mathscr{S}_i^h$) cells. For moderate problem sizes, this allows us to explicitly compute and store $\mathbf{J}(\boldsymbol{m})$ and to solve the Gauss-Newton system (5a) faster and more accurately using PCG than we could afford if we had to re-compute the sensitivities for every matrix–vector product at every PCG step.

NUMERICAL EXAMPLE

We demonstrate our approach with a synthetic VTEM data set. The survey covers an area of 12.6 km × 6.2 km with 4064 measurement locations that are spaced 100/200 m apart in x/y-direction. The transmitters and receivers are placed 40 m above ground. After the current is shut off at $t = 0$, 18 time channels are recorded between 0.2 ms and 9.2 ms. The global inverse problem mesh $\mathscr{S}^H$ contains 963 775 cells (Fig. 1a). We used 1024 local forward problem meshes $\mathscr{S}_i^h$ which accommodate 3 to 4 transmitter–receiver pairs each and contain 6770 to 10 802 cells (Fig. 2b). This is a reduction in mesh size by a factor of 100.

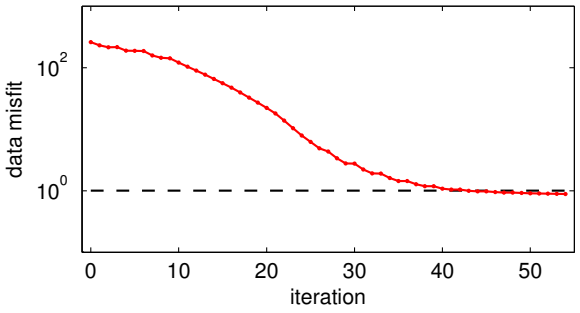

Figure 3. Convergence history of data misfit as function of Gauss-Newton iterations. The regularization parameter is reduced every three iterations. The dashed line indicates the data misfit of the ground truth.

Synthetic data was generated for a random earth model (Figs 2a, c) and sucessfully inverted (Figs 2b, d). The convergence history of data misfit and model smoothness are shown in Fig. 3. Even calculating and storing all 73 152 columns of the sensitivity matrix, we were able to run this example on a single node of our cluster using 12 parallel instances of MATLAB.

REFERENCES

Cox, L. H., & Zhdanov, M. S. (2008). Advanced computational methods of rapid and rigorous 3-D inversion of airborne electromagnetic data. *Commun. Comput. Phys.*, *3*, 160–179.

Günther, T., Rücker, C., & Spitzer, K. (2006). Three-dimensional modelling and inversion of dc resistivity data incorporating topography – II. Inversion. *Geophys. J. Int.*, *166*(2), 506–517.

Haber, E., & Heldmann, S. (2007). An OcTree multigrid method for quasi-static Maxwell's equations with highly discontinuous coefficients. *J. Comput. Phys.*, *65*, 324–337.

Haber, E., Oldenburg, D., & Shektman, R. (2007). Inversion of time domain 3D electromagnetic data. *Geophys. J. Int.*, *132*, 1324–1335.

Horesh, L., & Haber, E. (2011). A second order discretization of Maxwell's equations in the quasi-static regime on OcTree grids. *SIAM J. Sci. Comput.*, *33*, 2805–2822.

Schwarzbach, C., Börner, R.-U., & Spitzer, K. (2011). Three-dimensional adaptive higher order finite element simulation for geo-electromagnetics—a marine CSEM example. *Geophys. J. Int.*, *187*, 63–74.

Schwarzbach, C., & Haber, E. (2013). Finite element based inversion for time-harmonic electromagnetic problems. *Geophys. J. Int.*. (to appear)